Marine and Petroleum Geology 28 (2011) 439–449

Contents lists available at ScienceDirect

Marine and Petroleum Geology

journal homepage: www.elsevier.com/locate/marpetgeo

In-situ gas hydrate hydrate saturation estimated from various well logs at the Mount Elbert Gas Hydrate Stratigraphic Test Well, Alaska North Slope

M.W. Lee*, T.S. Collett

U.S. Geological Survey, Box 25046, MS-939 Denver Federal Center, Denver, Colorado 80225, USA

ARTICLE INFO

Article history:
Received 5 March 2009
Received in revised form
12 May 2009
Accepted 30 June 2009
Available online 8 July 2009

Keywords:
Gas hydrate
Saturation
Mount Elbert
Well logs
Rock physics model

ABSTRACT

In 2006, the U.S. Geological Survey (USGS) completed detailed analysis and interpretation of available 2-D and 3-D seismic data and proposed a viable method for identifying sub-permafrost gas hydrate prospects within the gas hydrate stability zone in the Milne Point area of northern Alaska. To validate the predictions of the USGS and to acquire critical reservoir data needed to develop a long-term production testing program, a well was drilled at the Mount Elbert prospect in February, 2007. Numerous well log data and cores were acquired to estimate in-situ gas hydrate saturations and reservoir properties.

Gas hydrate saturations were estimated from various well logs such as nuclear magnetic resonance (NMR), P- and S-wave velocity, and electrical resistivity logs along with pore-water salinity. Gas hydrate saturations from the NMR log agree well with those estimated from P- and S-wave velocity data. Because of the low salinity of the connate water and the low formation temperature, the resistivity of connate water is comparable to that of shale. Therefore, the effect of clay should be accounted for to accurately estimate gas hydrate saturations from the resistivity data. Two highly gas hydrate-saturated intervals are identified – an upper ~43 ft zone with an average gas hydrate saturation of 54% and a lower ~53 ft zone with an average gas hydrate saturation of 50%; both zones reach a maximum of about 75% saturation.

Published by Elsevier Ltd.

1. Introduction

Gas hydrates, or clathrates, are ice-like crystalline solids composed of water molecules surrounding gas molecules. In-situ physical characteristics of gas hydrate-bearing sediments have been investigated extensively because of their widespread occurrence in most of the world oceans and in permafrost regions (Kvenvolden, 1993) and their recognition as a negative feedback control on global temperature fluctuations (Archer, 2007), as a potential energy resource (Ruppel, 2007), and as a factor in seafloor stability and safety issues (Nixon and Grozic, 2007).

Under the Methane Hydrate Research and Development Act of 2000 (renewed in 2005), the U.S. Department of Energy (DOE) funds laboratory and field research on both Arctic and marine gas hydrates. Among the current Arctic studies, BP Exploration Alaska, Inc. (BPXA) and the DOE have undertaken a project to characterize, quantify, and determine the commercial viability of gas hydrates and associated free gas resources in the Prudhoe Bay, Kuparuk River, and Milne Point field areas on the Alaska North Slope.

In 2005, extensive analysis of BPXA's 3-D seismic data and the integration of that data with existing well log data (enabled by collaborations with the U.S. Geological Survey (USGS), the Bureau of Land Management, and IS Interpretation Services, Inc.), resulted in the identification of more than a dozen discrete and mappable gas hydrate accumulations within the Milne Point area (Inks et al., 2009). Because the most favorable of those targets was a previously undrilled, fault-bounded accumulation, BPXA and the DOE decided to drill a vertical stratigraphic test well at that location (named the "Mount Elbert" prospect) to acquire critical reservoir data needed to develop a long-term production testing program.

The BPXA-DOE-USGS Mount Elbert Gas Hydrate Stratigraphic Test Well (the "Mount Elbert Well") was drilled in the Milne Point area on the Alaska North Slope in 2007 and yielded one of the most comprehensive datasets yet compiled on naturally occurring gas hydrates. The coring team processed cores on site, and collected subsamples for analyses of pore water geochemistry, microbiology, gas chemistry, and physical, petrophysical, and thermal properties. After coring, the well was reamed to a diameter of 0.222 m (8.75 in), deepened to a depth of 915 m (3000 ft), and was surveyed with a research-level wireline logging program, including magnetic resonance and dipole acoustic logging, resistivity scanning, borehole electrical imaging, and advanced geochemistry logging.

Well logs have been used extensively to characterize in-situ gas hydrate-bearing sediments (GHBS) including saturations (e.g., Collett, 2000, 2002; Guerin et al., 1999; Helgerud et al., 1999; Hyndman et al., 2001; Lee and Collett, 2005). High quality well logs

* Corresponding author. Tel.: +1 303 236 5753; fax: +1 303 236 8822.
E-mail address: mlee@usgs.gov (M.W. Lee).

0264-8172/$ – see front matter Published by Elsevier Ltd.
doi:10.1016/j.marpetgeo.2009.06.007

acquired at the Mount Elbert Well provided a unique opportunity to accurately characterize the properties of naturally occurring GHBS and to assist in assessing gas hydrate as a potential energy resource on the Alaska North Slope. The purpose of this study is to analyze and accurately estimate in-situ gas hydrate saturations using various well logs such as nuclear magnetic resonance (NMR), P- and S-wave velocity, and electrical resistivity logs along with gamma and density logs, measured salinity and temperature data. Two highly gas hydrate-saturated reservoirs with gas hydrate saturations of about 60–75% of the pore space were identified from various well logs at the Mount Elbert well. These data were also used to refine rock physics models to accurately predict in-situ physical properties of GHBS.

2. Well log analysis

Downhole well logs can be used to characterize physical properties of GHBS and to estimate in-situ gas hydrate saturations. Well logs used in this study are gamma, density, NMR porosity, Dipole Sonic Imager (DSI) sonic (P- and S-wave velocity logs), and deep resistivity logs. A segment of the well logs showing characteristic log responses for highly saturated GHBS is shown in Fig. 1. Two gas hydrate reservoirs penetrated in the Mount Elbert well were identified on the basis of high resistivity, high P- and S-wave velocities with low NMR porosity and are denoted as hydrate units C and D in Fig. 1 according to nomenclature used by Collett (2002).

Measurements such as density and NMR porosity depend only on the bulk volume of gas hydrate in the pore space. However, other measurements such as elastic velocities and resistivity depend on the pore scale interactions between the gas hydrate and porous media as well as the bulk volume of gas hydrates. Therefore, gas hydrate estimates from the NMR log can serve as reference saturation, and enable us to assess the accuracy of gas hydrate saturations estimated from other well logs, and to refine the rock physics model.

Clay volume plays an important role in modeling elastic velocities and electrical resistivity. Clay volume content is calculated from the shale volume by multiplying by 0.6 (Hearst et al., 2000) and the shale volume is calculated from the gamma log using the formula pertinent to Tertiary clastics with $G_{cn} = 10$ (API units) and $G_{sh} = 120$ (API units), where G_{cn} and G_{sh} are the gamma ray log responses in a zone considered to be clean and the log response in a shale bed (Western Atlas International Inc., 1995), respectively. A detailed description of the shale volume estimated from the gamma log is given in Appendix A.

In addition to the six well logs described above, salinity and temperature data are used in this study and are shown in Table 1.

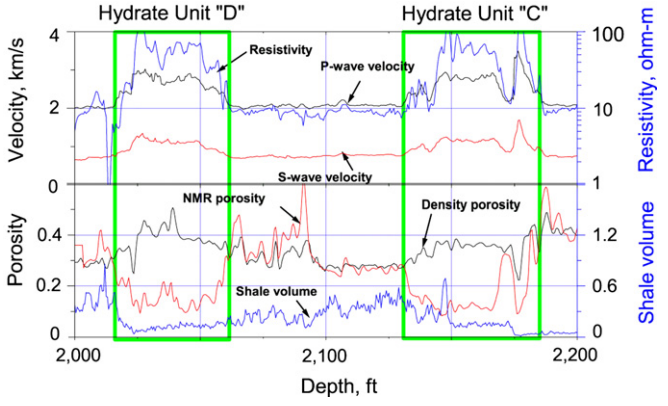

Fig. 1. Well logs for depth interval 2000–2200 ft, showing two gas hydrate-bearing portions of units C and D penetrated in the Mount Elbert well, northern Alaska.

Table 1
Measured salinity (from Torres et al., 2011) and temperature at the Mount Elbert well, Northern Alaska.

Depth, ft	Salinity, ppt	Temperature, °C	Depth, ft	Salinity, ppt	Temperature, °C
1996.79	7	2.015	2237.75	4.5	4.53
2002.96	7	2.079	2245	4.5	4.622
2018.67	7.5	2.215	2259.92	5	4.773
2030.08	2.5	2.341	2262.25	5	4.777
2033.25	2.5	2.373	2271.25	5.5	4.864
2045.17	3.5	2.493	2299.83	5.5	5.13
2056.96	3.5	2.583	2320.42	4.5	5.226
2069.83	5	2.737	2327.92	4	5.377
2082	5	2.846	2342.5	5	5.497
2087.75	5	2.902	2345.67	5	5.518
2105.5	5.5	3.116	2363.75	4.5	5.701
2115.29	6	3.23	2369.75	5	5.774
2127.33	6	3.358	2402.67	4	6.171
2150.67	2.5	3.648	2411.42	4	6.305
2157.54	4	3.757	2426.5	3.5	6.393
2161.88	3.5	3.77	2429.92	4	6.412
2167.46	3.5	3.893	2448.42	3.5	6.594
2175.58	4.5	3.91	2458.17	3.5	6.726
2182.08	2.5	3.986	2479.67	4.5	6.89
2192.54	4.5	4.013	2487.08	4.5	6.963
2207.58	5.0	4.236	2492.25	4.0	7.013
2213.38	4.5	4.285			
2231.75	4.5	4.514			

3. Log measurements controlled only by gas hydrate content

3.1. Density

The bulk density of GHBS (ρ_b) can be written as

$$\rho_b = \rho_{ma}(1-\phi) + \rho_w\phi(1-C_h) + \rho_h\phi C_h, \quad (1)$$

where ϕ is the total porosity, ρ_{ma}, ρ_w, and ρ_h are densities of grains, water, and gas hydrate, respectively, and C_h is the gas hydrate saturation in the pore space. The grain density of 2.67 g/cm^3, which is based on the core density (Winters et al., this volume), is used to compute the porosity from equation (1).

3.2. NMR

The NMR porosity (ϕ_{NMR}) measures the pore space occupied only by water (bound, capillary, and free water) and is given by the following equation:

$$\phi_{\mathrm{NMR}} = \phi(1-C_h) \quad (2)$$

From equations (1) and (2)

$$\phi = \frac{\phi_D + \lambda_h\phi_{\mathrm{NMR}}}{1+\lambda_h} \quad (3)$$

$$C_{\mathrm{h}} = \frac{\phi - \phi_{\mathrm{NMR}}}{\phi} \quad (4)$$

where

$$\lambda_h = \frac{\rho_w - \rho_h}{\rho_{ma} - \rho_w} \text{ and } \phi_D = \frac{\rho_{ma} - \rho_b}{\rho_{ma} - \rho_w} \quad (5)$$

Note that ϕ_D is the conventional density porosity derived using a two-component system (matrix and water) and ϕ_{NMR} is the same as the water-filled porosity that is defined as $\phi_w = (1 - C_h)\phi$. The porosity given in equation (3) is total porosity, which is the space occupied by water and gas hydrate in the pore space. "Total porosity" and porosity are used interchangeably in this paper.

The gas hydrate saturations estimated from the NMR and density porosity do not depend on the model or parameters, so the

accuracy of the estimation depends only on the accuracy of NMR and density logs. Therefore, it is assumed that gas hydrate saturations estimated from the NMR and density logs are the most accurate in-situ gas hydrate saturations and the accuracy of other methods can be evaluated using the NMR saturations as reference saturations.

4. Log measurements controlled by pore scale interaction

4.1. Electrical resistivity

The electrical resistivity of water-saturated sediments (R_o) can be expressed using the Archie equation (Archie, 1942) in the following way:

$$R_o = \frac{aR_w}{\phi^m} \tag{6}$$

where R_o is the formation resistivity of water-saturated sediment, R_w is the resistivity of the connate water, a and m are Archie constants, and ϕ is the porosity. Archie constants a and m can be derived empirically; m is commonly called the cementation factor. These a and m values depend on the interaction between the host sediments and gas hydrate in the porous medium. Equation (6) indicates that a plot of log ϕ relative to log R_o is linear and the slope is given by m if R_w is constant throughout the interval being analyzed or if the formation factor (FF), which is defined as FF $= R_o/R_w$, is used.

The water saturation (S_w) in the formation from the resistivity log value for sediments having hydrocarbons is given by Archie (1942) as

$$S_w = \left(\frac{aR_w}{\phi^m R_t}\right)^{1/n}, \tag{7}$$

where n is an empirically derived parameter close to 2 and R_t is the formation resistivity with gas hydrate or other hydrocarbons. The parameter n, depending on the reservoir lithology, varies between 1.715 (unconsolidated sediment) and 2.1661 (sandstone); is typically 1.9386 (Pearson et al., 1983) and $n = 2$ is used in this study.

The resistivity of connate water can be calculated using Arp's formula (Arp, 1953), if the salinity and temperature of the formation water are known. Arp's formula is $R_{w2} = R_{w1}(T_1 + 7)/(T_2 + 7)$ where R_{w1} and R_{w2} are water resistivities at Fahrenheit temperatures at T_1 and T_2, matched by laboratory measurement and subsurface formation conditions, respectively. Fig. 2 shows the calculated R_w from the measured salinity and temperature along with measured electrical resistivity for the Mount Elbert well. Note that the average R_w for the interval between 2000 and 2500 ft (609 to 762 m) is about 2 Ω-m except for two intervals with much higher resistivities, which reflect low salinity at low temperature. For comparison, R_w at the Mallik 5L-58 well, Western Canada, is about 0.45 Ω-m (Collett and Lee, 2005) and at Keathley Canyon, Gulf of Mexico, it is about 0.2 Ω-m (Lee and Collett, 2008). The zones where R_w is greater than approximately 3 Ω-m in Fig. 2 correspond to the hydrate-bearing portions of units C and D (Collett, 2002) and these zones were caused by freshening of pore water from the dissociation of gas hydrate. Consequently, the calculated resistivity greater than about 2 Ω-m in Fig. 3 does not represent in-situ resistivity of pore water.

Fig. 3 shows the relation between the formation factor calculated using the R_w and resistivity shown in Fig. 2 and density porosity for the water-saturated interval between 2200 and 2400 ft (670 to 732 m). The relation shown in Fig. 3 yields the Archie parameter $a = 1.7$ and $m = 1.0$ for water-saturated sediments. Fig. 2

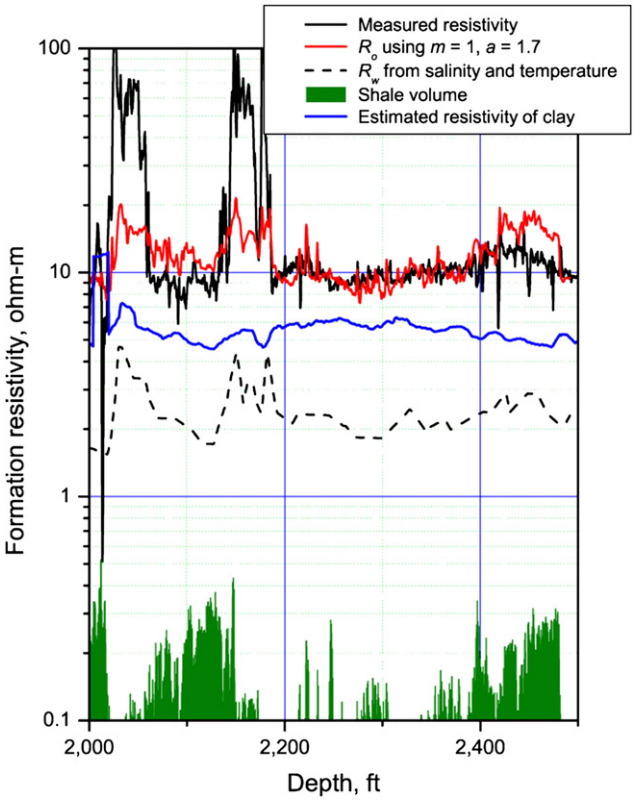

Fig. 2. Plot showing measured electrical resistivity with shale volume calculated from gamma ray log, resistivity of pore water calculated using salinity and temperature, estimated resistivity of clay, and baseline resistivity calculated from porosity and resistivity of connate water (R_w) with the Archie parameters $a = 1.7$ and $m = 1$.

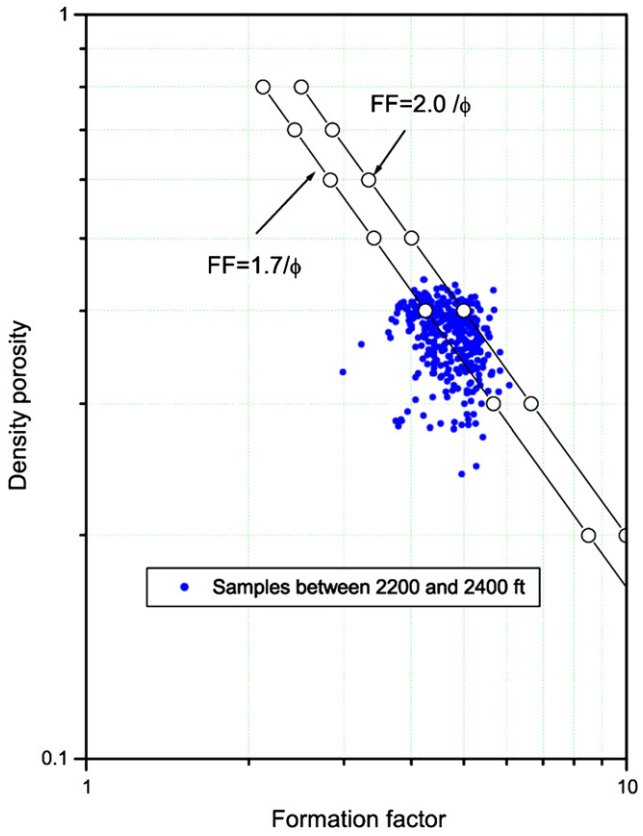

Fig. 3. Relation between formation factor and density porosity for depth interval between 2200 and 2400 ft.

also shows the calculated R_o using density porosity, calculated R_w, and equation (1) with $a = 1.7$ and $m = 1$. Fig. 2 indicates that the calculated R_o agrees well with the measured resistivity for cleaner intervals, whereas the calculated R_o is higher than the measured resistivity where significant amount of shale exists such as intervals between 2050 and 2150 ft (625 to 655 m) and between 2400 and 2440 ft (732 to 744 m). This implies that the clay effect on resistivity may be significant at the Mount Elbert well, partly because of the high resistivity of connate water. Also note that the calculated R_o for hydrate Units "C" and "D" are much higher than those of the adjacent sediments (Fig. 2) due to high R_w caused by the freshening of pore water due to gas hydrate dissociation as mentioned previously.

The effect of clay on the formation resistivity can be corrected using various shaly sand correction methods (Worthington, 1985). Lee and Collett (2006) proposed a method in which the Archie parameters a and m are a function of clay content. The essence of this method is that the estimates of a and m reflect the contribution of clay on the sediment's resistivity in such a way that as the clay content increases, a increases and m decreases. Therefore, a and m are a function of clay content. It assumes that the electrical conductivity of an aggregate of conductive particles saturated with a conducting electrolyte can be represented by resistivity elements in parallel (Wyllie and Southwick, 1954). Therefore, the effect of clay in sediments can be formulated in the following way (Simandoux, 1963):

$$\frac{1}{R_o} = \frac{1}{a_c\phi^{-m_c}R_w} + \frac{(1-\phi)C_v}{R_c} \equiv \frac{1}{FR_w} + Q_c \tag{8}$$

where F is a formation factor for clean sands ($F = a_c\phi^{-m_c}$), a_c and m_c are Archie parameters appropriate for clean sand, C_v is the volume fraction of clay in solid matrix, R_c is the resistivity of the clay, and Q_c is the effective clay conductivity, which is estimated as (Lee and Collett, 2006):

$$Q_c = \frac{\phi^m(a_c - a\phi^{m_c-m})}{a_c a R_w} \tag{9}$$

The water saturation can be estimated by

$$S_w = \left(\frac{a_c R_w(1 - R_t Q_c)/R_t}{\phi^{m_c}}\right)^{1/n} \tag{10}$$

Note that when $a = a_c$ and $m = m_c$, $Q_c = 0$ and equation (10) reduces to equation (7) and the gas hydrate saturation is given by $C_h = 1 - S_w$.

A linearity condition between log ϕ and log R_o is essential for the proposed method to be effective. This condition is satisfied if the conductivity contribution from the clay is less than about 40% of the conductivity contributed from the pore fluid (Lee and Collett, 2006). Also, the Archie parameters a and m for the clean sand are constrained by the following equation (Lee and Collett, 2006):

$$m + \ln(a_c/a)/\ln\phi < m_c < m + \ln(a_c/a - S_w^2/a)/\ln\phi \tag{11}$$

Fig. 4 shows gas hydrate saturations estimated from the resistivity both without (Fig. 4A) and with a shaly sand correction (Fig. 4B) using $a = 1.7$, $m = 1$, $a_c = 1$, and $m_c = 1.6$. It is assumed that $a = 1.7$ and $m = 1$ are appropriate parameters for sediments with 13% shale content and a and m are linearly interpolated with respect to shale content to calculate Q_c in equation (9). Equation (11) yields $1.55 < m_c < 1.65$ using $a = 1.7$, $m = 1$, $a_c = 1$, $\phi = 0.38$, and $S_w = 0.3$; consequently $m_c = 1.6$ was chosen for the shaly sand correction. Gas hydrate saturations estimated from the resistivity without a shaly sand correction are smaller than those from the NMR, whereas those estimated with a shaly sand correction are comparable to those estimated from NMR in unit D and slightly higher for unit C.

4.2. Acoustic velocities

The relation between gas hydrate and velocities can be modeled using the three-phase Biot-Type equation (TPE) (Leclaire et al., 1994; Carcione and Tinivella, 2000; Lee, 2007) by assuming that gas hydrate acts as a load-bearing component of the sediments.

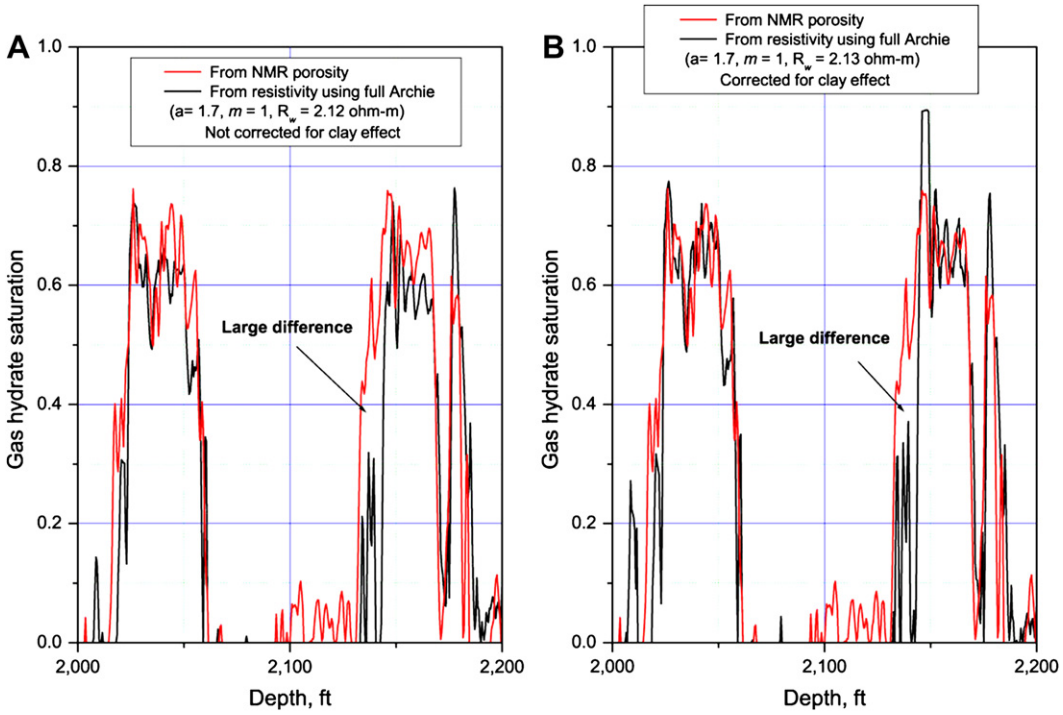

Fig. 4. Gas hydrate saturations estimated from the electrical resistivity with saturations estimated from the NMR log. A) Without shaly sand correction. B) With shaly sand correction.

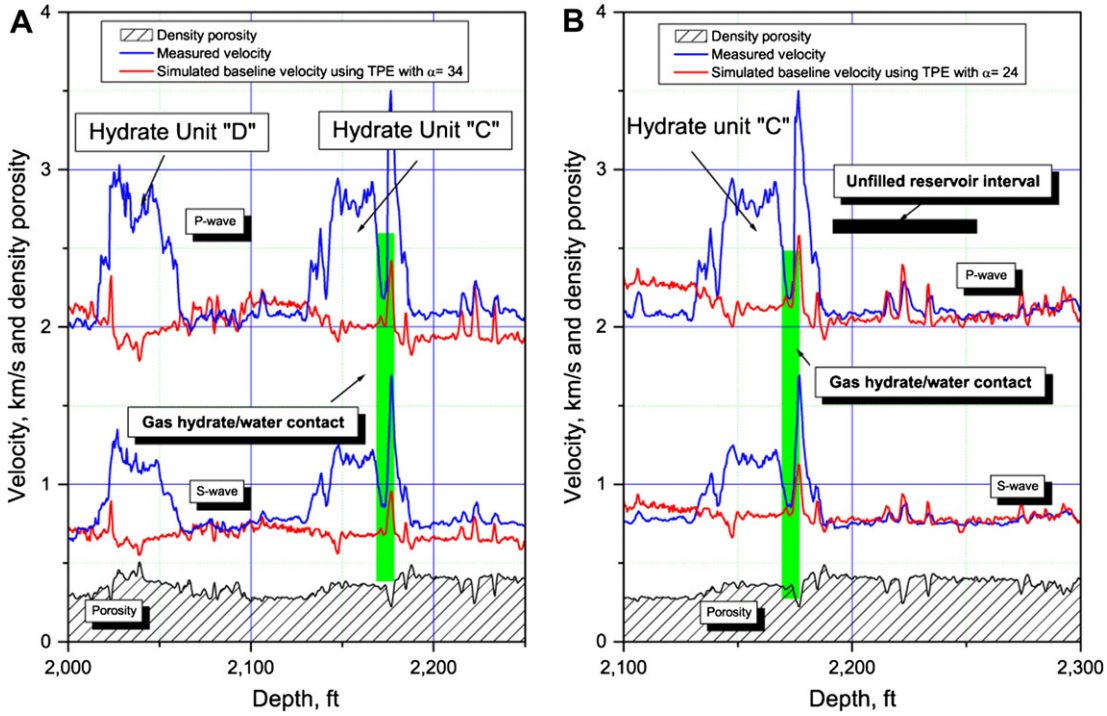

Fig. 5. Calculated baseline P- and S-wave velocities with measured P- and S-wave velocity and density porosity. A) Using the Biot-Gassmann theory (BGT) with the consolidation parameter $\alpha = 34$. B) Using BGT with the consolidation parameter $\alpha = 24$.

In this paper, the simplified TPE (Lee, 2008) is used to calculate velocities of GHBS. The P-wave velocity (V_p) and the S-wave velocity (V_s) of the GHBS can be calculated from the following:

$$V_p = \sqrt{\frac{k + 4\mu/3}{\rho_b}} \text{ and } V_s = \sqrt{\frac{\mu}{\rho_b}} \tag{12}$$

where k and μ are the bulk and shear moduli of the GHBS, and ρ_b is the bulk density of GHBS given by $\rho_b = \rho_{ma}(1-\phi) + \rho_w\phi(1-C_h) + \rho_h\phi C_h$.

The bulk and shear moduli of GHBS using the simplified TPE is given by Lee (2008):

$$\begin{aligned} k &= K_{ma}(1-\beta_p) + \beta_p^2 K_{av} \\ \mu &= \mu_{ma}(1-\beta_s) \end{aligned} \tag{13}$$

with

$$\frac{1}{K_{av}} = \frac{(\beta_p - \phi)}{K_{ma}} + \frac{\phi_w}{K_w} + \frac{\phi_h}{K_h},$$
$$\beta_p = \frac{\phi_{as}(1+\alpha)}{(1+\alpha\phi_{as})}, \text{ and } \beta_s = \frac{\phi_{as}(1+\gamma\alpha)}{(1+\gamma\alpha\phi_{as})}.$$

where α is the consolidation parameter (Pride et al., 2004; Lee, 2005a) with $\gamma = 1 + 2\alpha/1 + \alpha$ and $\phi_{as} = \phi_w + \varepsilon\phi_h$. Lee (2007) and Lee and Waite (2008) recommended $\varepsilon = 0.12$ for modeling velocities of GHBS. Ignoring the attenuation, the velocities calculated using the simplified TPE and the original TPE at low frequency such as the logging frequency are virtually identical, except that the simplified TPE is computationally much simpler to compute velocities.

K_{ma}, K_w, and K_h in equation (13) are the bulk modulus of the grains, water, and gas hydrate, respectively, and μ_{ma} is the shear modulus of the grains. Note that K_{ma} and μ_{ma} include the bulk and shear moduli of gas hydrate and are computed using Hill's (1952) average formula as shown in Helgerud et al. (1999). In the case that there is no gas hydrate in the pore space, apparent porosity ϕ_{as} is equal to porosity ϕ and equation (13) is an identical form for the bulk modulus derived by the Biot-Gassmann theory (BGT). For details of TPE for GHBS, consult Lee and Waite (2008) and Lee (2007, 2008).

Fig. 5 shows the baseline (baseline is defined as any property expected when there is no gas hydrate in the pore) velocities calculated from the density porosity using TPE with $\alpha = 34$, clay volume content calculated from the shale volume as shown in Fig. 2, and elastic constants shown in Table 2. The calculated P- and S-wave velocities are similar to the measured velocities for non-reservoir intervals and much smaller at the reservoir intervals. The much larger measured velocities in the reservoir intervals are due to gas hydrate.

Fig. 6 shows gas hydrate saturations estimated from P- and S-wave velocities using $\alpha = 34$ and $\varepsilon = 0.12$ (equation (13)). Saturations estimated from both P- and S-wave velocities are comparable to those from the NMR for units C and D. However, saturations estimated from the S-wave velocities are slightly higher than NMR-derived saturations for the non-reservoir interval near the 2125-ft depth.

5. Discussions

5.1. Clay effect on resistivity

In the case that the resistivity of connate water is comparable to that of clay, the effect of clay on electrical resistivity is significant.

Table 2
Constants used for the modeling modified from Lee (2002). Subscript "c" stands for clay.

$K_s = 38$ GPa	$\mu_s = 44$ GPa	$\rho_s = 2650$ kg/m^3
$K_c = 20.9$ GPa	$\mu_c = 6.85$ GPa	$\rho_c = 2580$ kg/m^3
$K_h = 6.41$ GPa	$\mu_h = 2.54$ GPa	$\rho_h = 910$ kg/m^3
$K_w = 2$ 0.29 GPa	$\mu_w = 0$	$\rho_w = 1000$ kg/m^3

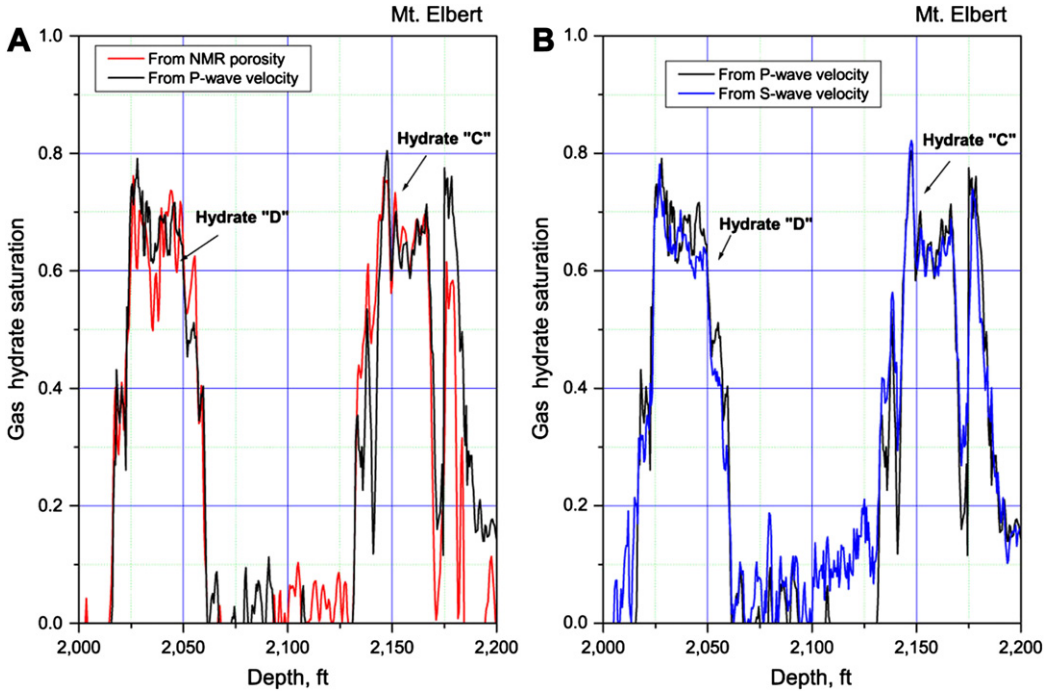

Fig. 6. Gas hydrate saturations estimated from the acoustic data with saturations estimated from the NMR log using three-phase Biot-type equation with the consolidation parameter $\alpha = 34$ for all depths. A) From the NMR log and the P-wave velocity. B) From the P- and S-wave velocities.

As shown in Fig. 2, the calculated R_o using the porosity and connate water resistivity overestimates the measured resistivity for intervals with high shale content. To derive accurate gas hydrate saturations, the resistivity due to conductive clay should be corrected using methods such as a dual-water model (Clavier et al., 1977) or a shaly sand model by Waxman and Smits (1968). In this paper, a simple method proposed by Lee and Collett (2006) is applied to qualitatively evaluate the effect of clay. The resistivity of clay (R_c) estimated from Lee and Collett (2006) using equation (9) averages about 5 Ω-m, as shown in Fig. 2. The resistivity of shale in the range of 5 Ω-m was used by Miyairi et al. (1999) in analyzing the resistivity log for GHBS at the Mallik 2L-38 well in western Canada.

Lee and Collett (2006) presented a condition for the validity of their proposed method as:

$$R_c > \frac{(1-\phi)R_w C_v}{0.4\phi^2} \tag{14}$$

Using $R_w = 2.13$, $\phi = 0.38$, $C_v = 0.2$, the right side of equation (14) is ~4.5, which is slightly smaller than the estimate R_c shown in Fig. 2. Therefore, the estimated saturation may be inaccurate where the clay volume is greater than about 20% or porosity is small.

5.2. Baseline velocities

The baseline P- and S-wave velocities shown in Fig. 5A are about 10% less than the measured velocities for depths greater than ~2170 ft (~661 m). The gas hydrate saturations shown in Fig. 6 indicates that those estimated from velocities agree well with estimates based on the NMR porosity for depths less than ~2170 ft (661 m), implying that that baseline velocities calculated with TPE with $\alpha = 34$ are fairly accurate. The NMR log clearly indicates that the sediment at a depth of about 2170 ft (661 m), shown as the "gas hydrate-water contact" in Fig. 5, is water-saturated. However, the calculated baseline velocities are about 10% less than the measured velocities of water-saturated sediments.

Fig. 5B shows that the baseline P- and S-wave velocities calculated from TPE with $\alpha = 24$ agree well with measured velocities or water-saturated sediments as indicated as "unfilled reservoir interval" and "gas hydrate/water contact" in the plot. Fig. 5A and B indicate that the elastic properties of sediments change significantly crossing the gas hydrate/water contact. The smaller consolidation parameter α indicates a higher degree of consolidation (either higher compaction or slightly higher cementation). Therefore, the sediments below the gas hydrate/water contact are more firmly consolidated.

5.3. Rock physics model

The acoustic properties of GHBS strongly depend on how the gas hydrate interacts with the porous medium. If gas hydrate cements the sediment grains, a small amount of gas hydrate increases the elastic velocities significantly. However, if the gas hydrate acts as a load-bearing component of sediments, the increase of velocity with respect to gas hydrate is moderate. Recent studies favor the load-bearing model of gas hydrate (Kleinberg et al., 2005). Many load-bearing models have been proposed; for example, the effective medium theory (EMT) by Helgerud et al. (1999), the modified Biot-Gassmann theory by Lee (BGTL) (Lee, 2002, 2005b), and the three-phase Biot-type equation (TPE) by Lee (2007). Although the same load-bearing concept of gas hydrate is common to each theory, the rate of velocity changes with respect to gas hydrate depends on the model. Likewise the accuracy of gas hydrate saturation estimates depend on the theories used. Because those based on the NMR were available for this study, the log data provided an opportunity to test various rock physics models. A detailed comparison among BGTL, and TPE for velocities of GHBS at the Mallik-5L well in western Canada was given in Lee and Waite (2008).

Fig. 7A shows modeled velocities using TPE along with BGTL for GHBS with porosities ranging from 36 to 40%. All models used $\phi = 0.38$ and $C_v = 0.1$ with elastic constants shown in Table 2. At low

saturations, the modeled velocities using BGTL are less than those modeled using TPE, whereas at higher saturations above about 0.4, modeled velocities using TPE are less than those using BGTL. Fig. 7B shows the relation between the measured P-wave/S-wave velocity ratio and the predicted ratios from EMT, BGTL, and TPE. For all ranges of S-wave velocity, TPE predicts an accurate velocity ratio, whereas the prediction from BGTL is slightly higher. Consequently, it is concluded that TPE performs better than BGTL in modeling velocities of GHBS at the Mount Elbert well.

5.4. Various estimated saturations

Three different physical properties measured from three different logging tools are used to estimate the gas hydrate saturations at the Mount Elbert well. The estimated saturations show some variations, which may be caused by measurement error, differences in the depth of investigation, clay effect on both acoustic and resistivity logs, and (or) inadequate theory or parameters.

5.4.1. NMR and resistivity

Saturations estimated using the quick-look method with $R_o = 9$ Ω-m (not shown in Fig. 4) are almost identical to those estimated without the shaly sand correction using the full Archie equation with $a = 1.7$ and $m = 1$ that are shown in Fig. 4A. It is noted that the calculated baseline resistivity for units C and D shown in Fig. 2 is not accurate for estimating gas hydrate saturation when using the full Archie analysis, because the pore water freshening due to dissociation of gas hydrate is reflected in the calculated R_o. Therefore, a constant $R_w = 2.13$ Ω-m is used for the full Archie analysis. The accuracy of the quick-look method depends only on the R_o value. If a R_o value lower than 9 Ω-m is used, and the effect of clay on resistivity is considered, the estimates would be closer to those from the NMR for units C and D, although lower R_o values yield some gas hydrate saturations in the non-reservoir intervals. Considering the clay effect on the resistivity, the Archie parameters $a = 1.7$ and $m = 1$ are probably reasonable values in estimating gas hydrate saturations at the Mount Elbert well. As demonstrated in Fig. 4B, the gas hydrate saturations estimated by applying a shaly sand correction approaches those estimated from the NMR, although it overestimates in some places. It is emphasized that the method employed in this paper is less accurate if the shale volume is higher than about 20% in a sediment with 38% porosity and becomes less accurate as porosity decreases. However, the simple shaly sand correction method used in this paper demonstrates that the effect of clay should be accounted for, mainly because the resistivity of connate water is comparable to that of clay at the Mount Elbert well.

At the top of unit C, there are large differences in gas hydrate saturations estimated from NMR and resistivity with or without shaly sand correction (marked as "large difference" in Fig. 4). Estimations from the P- and S-wave velocities shown in Fig. 6 are in agreement with NMR-derived saturations. Therefore, the differences may be caused partly by the difference in the vertical resolution.

5.4.2. NMR and acoustic

Gas hydrate saturations estimated from P-wave velocities agree well with saturations estimated from the NMR log. Estimated based on S-wave velocities are generally accurate for units C and D, but are erroneous, on the order of 10–20%, in the depth interval 2100–2125 ft (640 to 648 m) (predominantly shale interval) where NMR and P-wave velocity show negligible saturations. In this interval, the calculated S-wave baseline velocities using TPE with $\alpha = 34$, shown in Fig. 5A, are smaller than the measured S-wave velocities, whereas the baseline P-wave velocities are slightly higher than the measured velocities. Also in this interval, measured and calculated P-wave velocities and the calculated S-wave velocities are almost constant, whereas the measured S-wave velocities increase slightly with depth (Fig. 5A). This implies that TPE may not be accurate for predominantly shale interval. Also, the clay content estimated from the gamma log presented in the previous section may not be accurate for this interval. The effect of clay on elastic velocities is

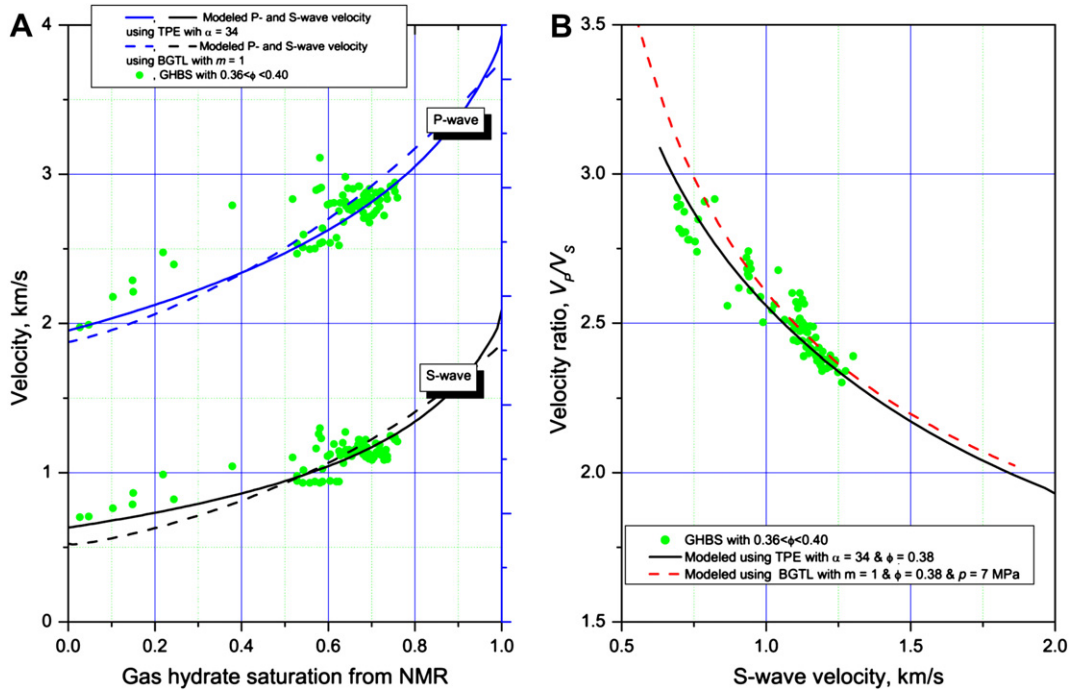

Fig. 7. Modeled and measured velocities. Measured velocities are from sediment having density porosity between 36 and 40% in the depth interval 2000–2200 ft. A) Relations between gas hydrate saturations estimated from the NMR log and P-wand S-wave velocity with modeled relation. B) Relation between measured S-wave and P-wave velocities with modeled relation.

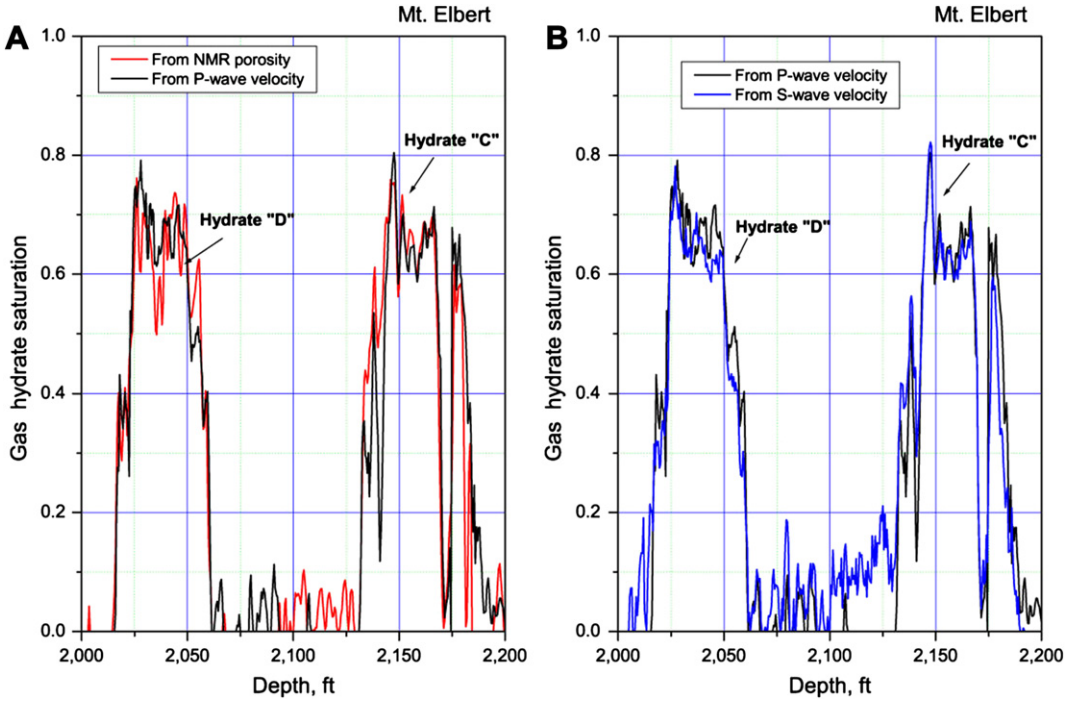

Fig. 8. Gas hydrate saturations estimated from the acoustic data with saturations estimated from the NMR log using the three-phase Biot-type equation with the consolidation parameter $\alpha = 34$ for depths less than 2170 ft and $\alpha = 24$ for depths greater than 2170 ft. A) From the NMR log and the P-wave velocity. B) From the P- and S-wave velocities.

complicated because clay may alter the pore structure such as the pore aspect ratios compared to clean sand intervals. The mismatch between the P- and S-wave velocities is possibly due to the inability of TPE to accurately model the clay effect on velocities. It is emphasized, however, that the TPE performs well for the sand reservoir intervals.

Fig. 6 also indicates that gas hydrate saturations estimated from the P- and S-wave velocities show 20–30% gas hydrate saturation for the interval shown as the gas hydrate/water contact, whereas saturations estimated from the NMR and resistivity (Fig. 5B) show no gas hydrate saturation; such errors were caused by inaccurate baseline velocities. The saturations estimated from elastic velocities using TPE with $\alpha = 34$ for depths less than 2170 ft (661 m) and with $\alpha = 24$ for depths greater than 2170 ft (661 m) are plotted in Fig. 8. Fig. 8 indicates that these saturations agree well with those estimated from the NMR log for depths greater than 2170 ft (661 m), implying that calculated baseline velocities using $\alpha = 24$ are appropriate for depths greater than 2170 ft (661 m) as shown in Fig. 5B. In summary, gas hydrate saturations estimated from various well logs agree with one another, approaching about 65–75% for both units C and D.

5.4.3. NMR and salinity

Salinity in the pore water has been used as a proxy for determining gas hydrate saturation, because dissociation of gas hydrate freshens the pore water (Paull et al., 1996; Cranston, 1999). Fig. 9A shows the measured salinity of the pore water (from Torres et al., 2011). To estimate saturations from the salinity data, an accurate baseline salinity should be determined. Fig. 9A shows two assumed baseline salinities and Fig. 9B shows the estimated saturation from the salinity data and a comparison with the NMR-derived saturations.

From the NMR and other logs, only hydrate Units "C" and "D" contain significant gas hydrate in the pore spaces, so well logs can be served to assess the accuracy of the salinity method in estimating saturations. Saturations estimated from the salinity data using two baseline salinities appear to be reasonable for hydrate Unit "D", but not for hydrate Unit "C"(Fig. 9B). Also, the non-reservoir interval around 2100 ft (661 m) contains a significant amount of gas hydrate from the salinity as opposed to the gas hydrate estimated from well logs. Comparing the estimated gas hydrate saturations and baseline salinity, it is evident that determining baseline salinity is not a simple matter at the Mount Elbert well. Fig. 9 implies that the salinity data can be effectively used as a qualitative indicator for the presence of the gas hydrate, but not as a quantitative estimation of the saturation.

5.5. Units C and D reservoirs

Fig. 10 shows gas hydrate saturations estimated from the NMR-density log along with volumes of free water and bound water. As indicated in Fig. 10A, unit D is completely filled with hydrate and is bounded by shales with a high bound water content (about 20% of the sediment volume). On the other hand, Fig. 10B indicates that unit C is partially filled and is bounded by shale at the upper contact and by clean sand with high capillary-bound water content in the lower bounding unit, indicated as a "barrier" in Fig. 10B at the lower boundary. The amount of bound water in the underlying "barrier" unit is more than 20% of the sediment's volume, similar to the bound water content at the upper and lower units bounding unit D.

Ignoring a small water-saturated interval shown as the gas hydrate/water contact in Fig. 5, the following observations can be made for the non-hydrate-bearing portion of the reservoir:

1. The volume of bound water in the non-hydrate-bearing portion of the sand interval in unit C is generally large compared to that in the hydrate-bearing sands. Considering the NMR, it appears that the bound water is mainly in the form of capillary-bound water, not clay-bound water. Consequently, the pore structure of the sands in the non-hydrate-bearing portion of the reservoir appears to differ substantially from that of the hydrate-bearing reservoir sands, which may be the result of sorting and grain size differences between the two sands and slight

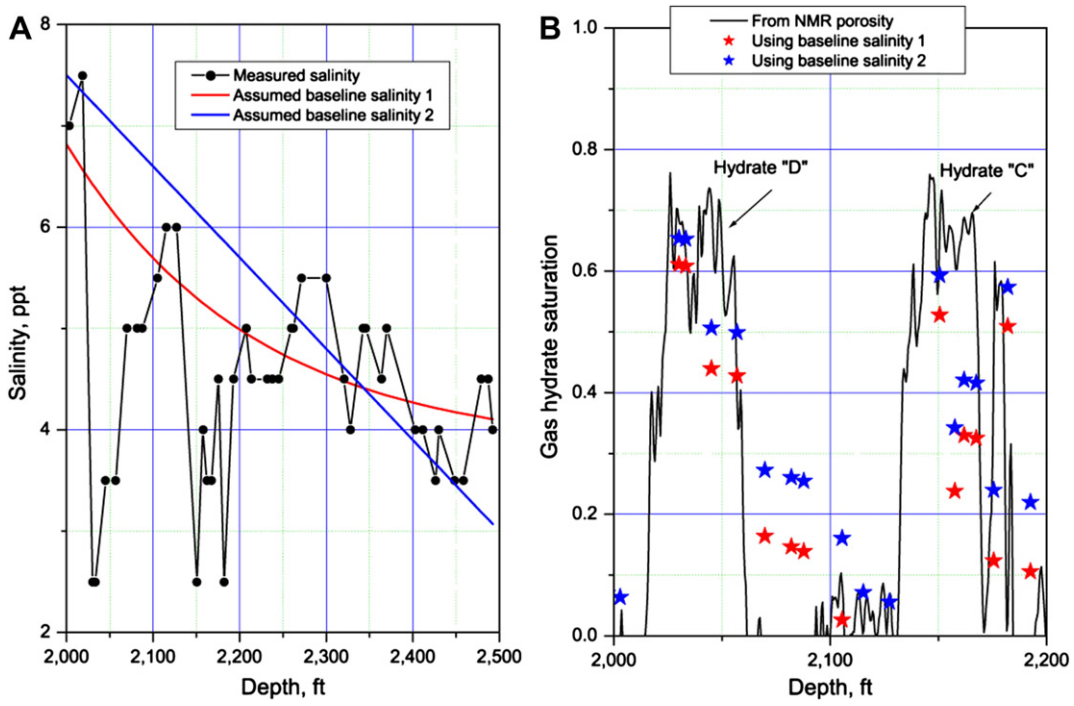

Fig. 9. Salinity and gas hydrate saturation. A) Measured salinity and two assumed baseline salinities. Baseline 1 assumes that the salinity decreases linearly with depth and baseline 2 assumes that the salinity decreases exponentially with depth. B) Gas hydrate saturations estimated from salinity data and NMR log.

cementation of the sand in the non-hydrate-bearing portion of the reservoir.

2. An average density porosity of 41% for the non-hydrate-bearing portion of the reservoir in the depth interval between 2180 and 2215 ft (664 to 675 m) is higher than that of the filled reservoir, which is 36% for depths between 2140 and 2170 (652 to 661 m) ft.
3. When using a constant consolidation parameter ($\alpha = 34$) to simulate P- and S-wave velocities without gas hydrate in the pore space, the difference between simulated and measured velocities changes abruptly at the lower contact of hydrate-bearing section in unit C (Fig. 5). Considering the high porosity of the non-hydrate-bearing portion of the reservoir, measured

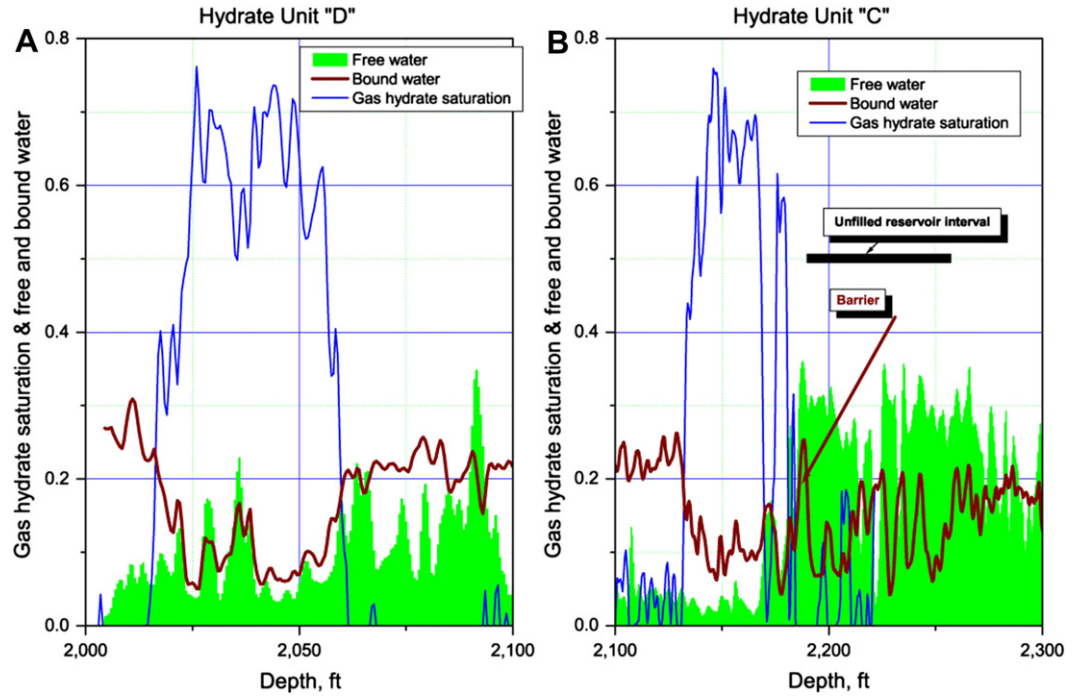

Fig. 10. Graph showing gas hydrate saturations estimated from the nuclear magnetic resonance (NMR) log, volume of free water, and volume of bound water. A) Hydrate Unit "D". B) Hydrate Unit "C".

baseline P- and S-wave velocities are anomalously high compared to those in the gas-hydrate-bearing portion of the reservoir. Because the porosity of the non-hydrate-bearing portion of the reservoir is higher than that of the hydrate-bearing portion of the reservoir, compaction is not the cause of the velocity changes across the lower hydrate contact. A slight increase in sediment cementation increases the elastic velocities of sediments significantly. Therefore, it appears that the sediments below the lower gas hydrate boundary are much more consolidated. For example, the consolidation parameter $\alpha = 34$ was used to model velocities for the sediment above the barrier and $\alpha = 24$ for sediment below the barrier. Lee (2005a) indicated that the value of the consolidation parameter increases as the degree of a sediment's consolidation decreases. A change from $\alpha = 34$ to $\alpha = 24$ at the boundary implies that the consolidation of sediments varies significantly at the boundary; however, drilling indicated no dramatic pore pressure changes near the barrier. Therefore, it appears that the change of baseline velocities across the boundary is probably caused by the change in the degree of consolidation, but at present no possible explanation is forthcoming.

6. Conclusions

To estimate gas hydrate saturations and assess the accuracy of different estimation methods, saturations calculated from the nuclear magnetic resonance (NMR) log are used as a reference and are compared to saturations estimated from other logs. On the basis of well log analysis at the Mount Elbert well, the following conclusions are drawn:

1) Two highly gas hydrate-saturated intervals are identified; the upper zone has a thickness of ~44 ft (13.4 m) ft with an average saturation of 54% and the lower zone has a thickness of 54 ft (16.5 m) ft with an average saturation of 50%; and both zones reach maximum saturations of about 75%.
2) The three-phase Biot-type equation (TPE) is preferable to modified Biot-Gassmann theory proposed by Lee (2002, 2005b) in modeling velocities of GHBS. TPE works for all ranges of gas hydrate saturations for clean reservoir intervals; however, TPE presented here may not be accurate for predominantly shale intervals.
3) The reservoir sands in unit D are fully filled, whereas the unit C reservoirs are only partially filled.
4) The salinity of connate water is small and the temperature at the reservoir is in the range of 2–4 °C. Consequently, the resistivity of connate water is large, about 2 Ω-m, and is comparable to the resistivity of clay, which is estimated at ~5 Ω-m. Therefore, the effect of clay on the electrical resistivity should be accounted for to accurately estimate gas hydrate saturations.
5) Freshening of pore water due to the dissociation of gas hydrate can be used only as a qualitative proxy for the presence of gas hydrate, because the baseline salinity in the Mount Elbert well has not been accurately determined.

Acknowledgements

We thank the Mount Elbert Science Team for the successful logging and coring program, and we appreciate Warren Agena and Tanya Inks for their many helpful comments and suggestions. This contribution was funded by the U. S. Geological Survey Energy Resources Program, the U. S. Department of Energy (under Interagency Agreement No. DE-AI21-92MC29214), and the U. S. Bureau of Land Management (under Interagency Agreement No. LAI-02-0015).

Appendix A

Estimating shale volume

Quantitative estimation of shale content using gamma log data assumes that radioactive minerals other than shales and clay are absent in sediment. The formula for estimating shale volume for Tertiary clastics using the gamma ray shale index (I_{gr}), which is calculated from the gamma log, is given by (Western Atlas International Inc., 1995; Hearst et al., 2000):

$$V_{sh} = 0.083\left(2^{3.7I_{gr}} - 1\right), \tag{A1}$$

with $I_{gr} = (G - G_{cn})/(G_{sh} - G_{cn})$, where V_{sh} is the shale volume, and G is the measured gamma log value, G_{cn} is the gamma log response in a zone considered clean (shale free), and G_{sh} is the log response in a shale bed. All log responses are in API units. For a given I_{gr}, the formula pertinent for the Mesozoic and older rocks, which is given by $V_{sh} = 0.33(2^{2I_{gr}} - 1)$, yields a higher shale volume than the equation for the Tertiary clastics. If it is assumed that $V_{sh} = I_{gr}$, which is a linear interpolation between gamma log and shale volume, it leads to overestimation of shale volume for Tertiary clastics.

Fig. A-1 shows the calculated V_{sh} using two different G_{sh} with the shale volume estimated from the X-ray powder diffraction (XRD) data (Winters et al., this volume). The shale volume using $G_{sh} = 110$ API appears to be more closely matched with the XRD data. In this paper, however, the shale volume calculated with $G_{sh} = 120$ API was used and this shale volume was estimated before the XRD data were available. Whether using the shale volume calculated with $G_{sh} = 110$ or 120 API doest not effect the results shown in this paper in any meaningful way and both V_{sh} can be effectively used in the well log analysis.

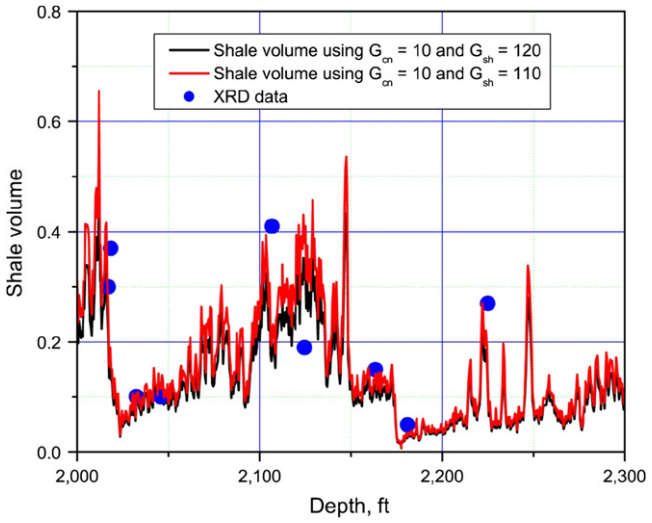

References

Archer, D., 2007. Methane hydrate stability and anthropogenic climate change. Biogeoscience 5, 5321–5344.
Archie, G.E., 1942. The electrical resistivity log as an aid in determining some reservoir characteristics. Journal of Petroleum Technology 1, 55–62.

Arp, J.J., 1953. The Effect of Temperature on the Density and Electrical Resistivity of Sodium Chloride Solutions, vol. 198. Petroleum Transaction, American Institute of Mining, Metallurgical, and Petroleum Engineers, pp. 327–330.
Carcione, J.M., Tinivella, U., 2000. Bottom-simulating reflectors: seismic velocities and AVO effects. Geophysics 65, 54–67.
Clavier, C., Coates, G., Dumanoir, J., 1977. The Theoretical and Experimental Bases for the Dual Water Model for the Interpretation of Shaly Sands: 52nd Annual Fall Technical Conference and Exhibition of the SPE of AIME, Denver, Colorado, October 9–12.
Collett, T.S., 2000. Quantitative Well-log Analysis of In-situ Natural Gas Hydrates. Ph.D. thesis. Colorado School of Mines, Golden, Colorado, 535 pp.
Collett, T.S., 2002. Energy Resource Potential of Natural Gas Hydrates, vol. 86, no. 11. AAPG Bulletin, pp. 1971–1992.
Collett, T.S., Lee, M.W., 2005. Electrical resistivity well log analysis of gas hydrate saturations in the JAPEX/JNOC/GSC et al. Mallik 5L-38 gas hydrate production research well. In: Dallimore, S.R., Collett, T.S. (Eds.), Scientific Results from the Mallik 2002 Gas Hydrate Production Research Well Program. Geological Survey of Canada Bulletin, vol. 585, p. 8. Mackenzie Delta, Northwest Territories, Canada.
Cranston, R.E., 1999. Pore-water geochemistry, JAPEX/JNOC/GSC Mallik 2L-38 gas hydrate research well. In: Dallimore, D.R., Uchida, T., Collett, T.S. (Eds.), Scientific Results from JAPEX/JNOC/GSC Mallik 2L-38 Gas Hydrate Research Well. Geological Survey of Canada Bulletin, vol. 544, pp. 165–175. Mackenzie Delta, Northwest Territories, Canada.
Guerin, G., Goldberg, D., Melsterl, A., 1999. Characterization of in situ elastic properties of gas hydrate-bearing sediments on the Blake Ridge. Journal of Geophysical Research 104, 17781–17796.
Hearst, J.R., Nelson, P.H., Paillett, F.L., 2000. Well Logging for Physical Properties — a Handbook for Geophysicists, Geologists and Engineers. John Wiley and Sons, New York, 484 pp.
Helgerud, M.B., Dvorkin, J., Nur, A., Sakai, A., Collett, T., 1999. Elastic-wave velocity in marine sediments with gas hydrates: effective medium modeling. Geophysical Research Letters 26, 2021–2024.
Hill, R., 1952. The elastic behavior of crystalline aggregates. Proceedings of the Physical Society, London A65, 349–354.
Hyndman, R.D., Spence, G.D., Chapman, R., Reidel, M., Edwards, R.N., 2001. Geophysical studies of marine gas hydrate in Northern Cascadia. In: Paul, C.K., Dillon, W.P. (Eds.), Natural Gas Hydrate: Occurrence, Distribution, and Detection. American Geophysical Union Geophysical Monograph, vol. 124, pp. 273–295.
Inks, T., Lee, M., Agena, W., Taylor, D., Collett, T., Hunter, R., Zyrianova, M., 2009. Prospecting for gas hydrate accumulations using 2D and 3D seismic data, Milne Point, North Slope, Alaska. In: Collett, T.S., Johnson, A., Knapp, C., Boswell, R. (Eds.), Natural Gas Hydrates; Energy Resource Potential and Associated Geologic Hazards. AAPG Memoir, vol. 89, pp. 1–29.
Kleinberg, R.L., Flaum, C., Collett, T.S., 2005. Magnetic resonance log of JAPEX/JNOC/GSC et al. Mallik 5L-38 gas hydrate production research well: gas hydrate saturation, growth habit, relative permeability. In: Dallimore, S.R., Collett, T.S. (Eds.), Scientific Results from the Mallik 2000 Gas Hydrate Production Research Well Program. Geological Survey of Canada Bulletin, vol. 585, p. 10. Mackenzie Delta, Northwest Territories, Canada.
Kvenvolden, K.A., 1993. A primer of gas hydrates. In: Howell, D.G. (Ed.), The Future of Energy Gases. U.S. Geological Survey, pp. 555–561. Professional Paper 1570.
Leclaire, P., Cohen-Tenoudji, F., Aguirre-Puente, J., 1994. Extension of Biot's theory of wave propagation to frozen porous media. Journal of Acoustical Society of America 96, 3753–3768.
Lee, M.W., 2002. Biot-Gassmann theory for velocities of gas-hydrate-bearing sediments. Geophysics 67, 1711–1719.
Lee, M.W., 2005a. Proposed Moduli of Dry Rock and Their Application to Predicting Elastic Velocities of Sandstones. U.S. Geological Survey, Scientific Investigation Report 2005–5119, p. 14.
Lee, M.W., 2005b. Well Log Analysis to Assist the Interpretation of 3-D Seismic Data at Milne Point, North Slope of Alaska. U.S. Geological Survey, Scientific Investigation Report 2005–5048, p. 18.
Lee, M.W., 2007. Velocities and Attenuations of Gas Hydrate-bearing Sediments. U.S. Geological Survey, Scientific Investigations Report 2007–5264, p. 11.
Lee, M.W., 2008. Models for Gas Hydrate-bearing Sediments Inferred from Hydraulic Permeability and Elastic Velocities. U.S. Geological Survey, Scientific Investigations Report 2008–5219, p. 15.
Lee, M.W., Collett, T.S., 2005. Assessments of gas hydrate concentrations estimated from sonic logs in the Mallik 5L-38 well, N.W.T., Canada. In: Dallimore, S.R., Collett, T.S. (Eds.), Scientific Results for Mallik 2002 Gas Hydrate Production Research Well Program. Geological Survey of Canada Bulletin, vol. 585, p. 10. Mackenzie Delta, Northwest Territories, Canada.
Lee, M.W., Collett, T.S., 2006. A Method of Shaly Sand Correction for Estimating Gas-hydrate Saturations Using Downhole Electrical Resistivity Log Data. U.S. Geological Survey, Scientific Investigation Report 2006–5121, p. 10.
Lee, M.W., Collett, T.S., 2008. Integrated analysis of well logs and seismic data at the Keathley Canyon, Gulf of Mexico, for estimation of gas hydrate concentrations. Marine and Petroleum Geology 25, 924–931.
Lee, M.W., Waite, W.F., 2008. Estimating pore-space gas hydrate saturations from well-log acoustic data. Geochemistry, Geophysics, Geosystems 9, 8. Q07008, 10, 1029/2008GC002081.
Miyairi, M., Akihisa, K., Uchida, T., Collett, T.S., Dallimore, S.R., 1999. Well-log interpretation of gas-hydrate-bearing formations in the JAPEX/JNOC/GSC Mallik 2L-38 gas hydrate research well. In: Dallimore, S.R., Uchida, T., Collett, T.S. (Eds.), Scientific Results from JAPEX/JNOC/GSC Mallik 2L-38 Gas Hydrate Research Well. Geological Survey of Canada Bulletin, vol. 544, pp. 281–293. Mackenzie Delta, Northwest Territories, Canada.
Nixon, M.F., Grozic, J.L., 2007. Submarine slope failure due to gas hydrate dissociation: a preliminary quantification. Canadian Geotechnical Journal 44, 314–325.
Paull, C.K., Matsumoto, R., Wallace, P.J., et al., 1996. In: Proceedings of ODP Initial Reports, 164: College Station, Texas, 459 pp.
Pearson, C.F., Halleck, P.M., McGuire, P.L., Hermes, R., Mathews, M., 1983. Natural gas hydrate deposit: a review of in-situ properties. Journal of Physical Chemistry 97, 4180–4185.
Pride, S.R., Berryman, J.G., Harris, J.M., 2004. Seismic attenuation to wave-induced flow. Journal of Geophysical Research 109, B01201. doi:10.1029/2003JB002639.
Ruppel, C., 2007. Tapping methane hydrates for unconventional natural gas. Elements 3, 193–199.
Simandoux, P., 1963. Dielectric Measurements on Porous Media; Application to the Measurement of Water-saturations, vol. 18. Revue de l'Institut Franscais du Petrole, Supplementary issue, pp. 193–215. (Translated text in shaly sand reprint volume, Society of Professional Well Log Analysts, Houston, pp. IV 97–124).
Torres, M.E., Collett, T.S., Rose, K.K., Sample, J.C., Agena, W.F., Rosenbaum, E.J., 2011. Pore fluid geochemistry from the Mount Elbert Gas Hydrate Stratigraphic Test Well, Alaska North Slope. Journal of Marine and Petroleum Geology 28 (2), 332–342.
Waxman, M.N., Smits, L.J.M., 1968. Electrical conductivities in oil-bearing shaly sands. Society of Petroleum Engineers Journal 8, 107–122.
Western Atlas International Inc., 1995. Introduction to Wireline Log Analysis. Western Atlas International Inc. (chapter 4), 312 pp.
Worthington, P.F., 1985. The evolution of shaly-sand concepts in reservoir evaluation. The Log Analyst (1), 23–40.
Wyllie, M.R.J., Southwick, P.F., 1954. An experimental investigation of the S.P. and resistivity phenomena in shaly sands. Journal of Petroleum Technology 6, 44–57.